

The redshift factor and the first law of binary black hole mechanics in numerical simulations

Aaron Zimmerman,¹ Adam G. M. Lewis,¹ and Harald P. Pfeiffer¹

¹*Canadian Institute for Theoretical Astrophysics, 60 St. George Street, Toronto, ON, M5S 3H8*

(Dated: May 30, 2022)

The redshift factor z is an invariant quantity of fundamental interest in Post-Newtonian and self-force descriptions of compact binaries. It connects different approximation schemes, and plays a central role in the first law of binary black hole mechanics, which links local quantities to asymptotic measures of energy and angular momentum in these systems. Through this law, the redshift factor is conjectured to have a close relation to the surface gravity of the event horizons of black holes in circular orbits. We propose and implement a novel method for extracting the redshift factor on apparent horizons in numerical simulations of quasi-circular binary inspirals. Our results confirm the conjectured relationship between z and the surface gravity of the holes and that the first law holds to a remarkable degree for binary inspirals. The redshift factor allows us to test analytic predictions for z in spacetimes where the binary is only approximately circular, giving a new connection between analytic approximations and numerical simulations.

Introduction.— The relativistic two body problem is of fundamental importance in both relativity theory and in the astrophysics of compact objects. Compact binaries emit gravitational radiation and spiral inward, eventually merging in a dynamic and nonlinear process; the end stages of this process are the most promising sources for gravitational waves and give a window into untested regimes of physics. The recent landmark detections of binary black hole mergers through gravitational waves [1–3] highlights both the sophistication of waveform models and the need for further improvements in order to search for and interpret gravitational wave signals. Current methods include post-Newtonian (PN) expansions in the slow velocity regime [4], self-force (SF) approximations [5] which apply to systems with high mass ratios, and direct numerical solutions [6–8] of the fully nonlinear problem beginning tens of orbits before merger. Each method has its limitations, and they are combined into effective one body (EOB) [9, 10] and phenomenological models [11] to produce full gravitational waveform predictions. In addition, connections and cross-comparisons between the different approaches yield deeper insights into each of them [12, 13]. Such insights are needed to deepen our understanding of general relativity and to maximize the scientific benefits of future gravitational wave observations.

Invariant quantities play a crucial role in these comparisons, since each method relies on computations in different gauges and uses various numerical codes. The invariant redshift factor z has proven essential in comparisons between analytic approximations, as first discussed in the context of binary systems which move on precisely circular orbits [14]. Such systems remain stationary in the corotating frame, resulting in a special helical symmetry embodied in a helical Killing vector (HKV) K^μ . In this context, the redshift factor allows for comparison of results obtained in various coordinate gauges [15, 16], and has played a central role in the development of PN

and EOB theory using SF results, e.g. [17–19].

For isolated black holes, the laws of black hole mechanics are relations between the area, angular momentum, and charges of the holes [20, 21]. These relations provide deep insights into the nature of classical black hole spacetimes, and when combined with quantum field theory they reveal the unexpected thermodynamic nature of black holes [22]. Modified laws of black hole mechanics exist in spacetimes with a HKV, interrelating properties of the orbiting bodies (self-gravitating fluid bodies or black holes) [23]. There is a compelling connection between the redshift factor z and these laws: when applied to HKV spacetimes in the PN and SF approximations, where stars and black holes are represented as test bodies, z enters into the laws as a generalized force, in direct analogy to the surface gravity of the approximated body [18]. With the help of z , these laws have played a growing role in PN [18, 24], SF [25, 26] and EOB [19, 27, 28] modeling of binary systems. These models then inform theoretical templates in use by Advanced LIGO [29] to enable detection and characterization of gravitational waves emitted by compact binaries [1, 30, 31].

The extension of redshift-based analyses to full numerical simulations of the field equations faces two problems. First, past comparisons have taken place in the context of conservative dynamics, where a HKV exists exactly, or in an averaged sense for eccentric orbits. However, in numerical simulations dissipation is always present, causing the black holes to inspiral and to break helical symmetry. Second, in analytic theory z is computed on particle worldlines, but numerical simulations deal with extended bodies whose interiors may even be excised from the computational domain, so that no worldline is available. Thus, while z has been used extensively to communicate between analytic methods, it has not been used to connect to numerical simulations. An important exception is the study of the related approximate relation

between the Bondi energy E_B and the Bondi angular momentum J_B , which has been tested using numerical simulations of binary inspiral [32–34].

This Letter reports the first application of redshift comparisons to numerical simulations. While quasi-circular binaries do not possess a strict HKV, their early inspiral can be approximated by adiabatic evolution through a sequence of circular orbits. As such, they should possess an approximate HKV in the spacetime region near the binary constituents. We discuss how the connection between the redshift factor and the surface gravity on black holes in the presence of a HKV can be used to define a normalized surface gravity and corresponding redshift factor for black holes. We then extract z from nonspinning binary black hole simulations and compare the numerical redshift factor to PN results. Finally, with our redshift factor we test the laws of binary black hole mechanics for quasi-circular orbits. We also validate the conjecture that the first law holds when dissipation is present, so long as the Arnowitt-Deser-Misner (ADM) mass and angular momentum are replaced with the corresponding Bondi quantities [18].

The first law of binary black hole mechanics and the redshift factor.— Consider a spacetime with a HKV K^μ containing one or more black holes. When the spacetime is asymptotically flat, we write $K^\mu = (\partial_t)^\mu + \Omega(\partial_\phi)^\mu$, where $(\partial_t)^\mu$ is the asymptotic Killing time measured by a set of inertial observers, $(\partial_\phi)^\mu$ is a spacelike vector with closed orbits of length 2π , and Ω is the orbital frequency of the Killing flow. The black holes have Killing horizons, with the tangents to their generators χ^μ equal to K^μ . The surface gravity κ of the hole is defined by the relation $\chi^\mu \nabla_\mu \chi^\nu = \kappa \chi^\nu$, and is constant on the horizon. We see that κ arises from the non-affine parameterization of χ^μ , which is normalized to equal K^μ . The overall normalization of K^μ is fixed by the vector $(\partial_t)^\mu$. In the case of a single rotating black hole, $(\partial_t)^\mu$ and $(\partial_\phi)^\mu$ are the usual timelike and axial Killing vectors of Kerr, Ω is the angular velocity of the horizon, and the spacetime obeys the famous laws of black hole mechanics [21].

More generally, HKV spacetimes obey the first law of binary mechanics. This law can be cast in terms of a Noether charge Q [23, 35], whose variations obey

$$\delta Q = \delta M - \Omega \delta J = \kappa_1 \frac{\delta A_1}{8\pi} + \kappa_2 \frac{\delta A_2}{8\pi}. \quad (1)$$

Here M and J are the ADM mass and angular momentum of the spacetime, and κ_i are the surface gravities defined by the generators of the Killing horizons of the black holes. The power of (1) lies in the fact that it connects local quantities defined on the black holes to asymptotic quantities, through the global vector field K^μ . Strictly speaking, both (1) and the required asymptotic flatness require that some conservative approximation to general relativity holds in the helically symmetric spacetime.

Next, consider spacetimes with point particles on cir-

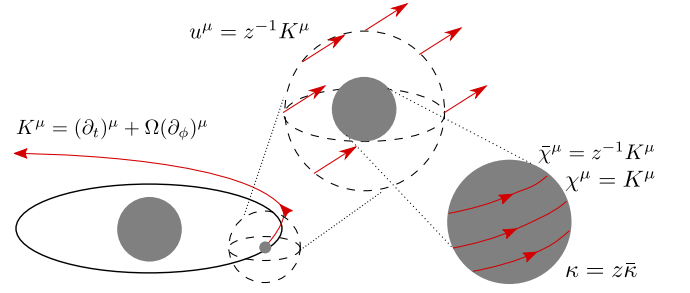


FIG. 1. Illustration of the connection between the redshift factor z and the surface gravity κ of a small black hole, using a matched asymptotic analysis of a HKV spacetime.

cular orbits. These particles model compact objects in the PN and SF approximations. The redshift factor z of a point particle moving with four-velocity u^μ is defined as $z = 1/u^t$, where t is the asymptotic Killing time entering K^μ . This redshift factor compares, in a certain effective metric, the clock rate of the particle to the clock rate at infinity, or equivalently the redshift of light emitted perpendicular to the particle’s motion. In this sense z is a well-defined observable for the particle, and is preserved by helically symmetric gauge transforms [14].

In [18] it is shown that a modified law of black hole mechanics exists for nonspinning point particles, which reads $\delta Q = z_1 \delta m_1 + z_2 \delta m_2$, with z_i and m_i the redshift factors and masses of the particles. Here, the redshift factor takes the role of the surface gravity of the black hole it replaces. These relations have been verified to high PN order and at leading order in SF for a corotating system [25], and have been used extensively to connect analytic approximations and waveform models, often by assuming they continue to hold at higher orders. The variational equations give rise to an integral relation,

$$Q = M - 2\Omega J = z_1 m_1 + z_2 m_2 = \kappa_1 \frac{A_1}{4\pi} + \kappa_2 \frac{A_2}{4\pi}. \quad (2)$$

This final relation is of primary interest to us: it shows how to connect local notions of the surface gravity to the redshift factor and the energy and angular momentum of the spacetime.

Surface gravity and the redshift factor.— Our first step is to make sense of z in a spacetime without a particle worldline on which to evaluate u^t . The first law (2) provides an explicit connection between surface gravity and the redshift factor: if we equate the masses m_i to the irreducible masses of the holes, $m_{\text{irr},i} = \sqrt{A_i/(16\pi)}$, then $\kappa_i = z_i/(4m_{\text{irr},i})$ and we have

$$\kappa_i = z_i \bar{\kappa}_i, \quad (3)$$

where $\bar{\kappa}$ is the surface gravity of an isolated, nonspinning hole. In the limit of infinite separation, $z_i \rightarrow 1$, and κ_i reduce to the expected values.

A heuristic derivation of Eq. (3) is given in Fig. 1, which depicts a matched asymptotic picture of a binary

black hole with masses m_1 and m_2 , and a small mass ratio $q = m_2/m_1$. The smaller hole is surrounded by a matching region which remains large compared to the hole, but becomes arbitrarily small in the point particle limit $q \rightarrow 0$. In the matching zone, we consider a family of comoving observers with four-velocity u^μ ; this velocity field must be parallel to K^μ by the symmetry, and becomes equal to the point particle velocity in the limit $q \ll 1$. Because $u^t = z^{-1}$ we have $u^\mu = z^{-1}K^\mu$. From the perspective of the matching zone observers, the small black hole is an isolated black hole immersed in an external tidal field [36]. These observers use their own asymptotic normalization on the HKV to define the tangents $\bar{\chi}^\mu = z^{-1}\chi^\mu$, and define their rescaled surface gravity through $\bar{\chi}^\mu \nabla_\mu \bar{\chi}^\nu = \bar{\kappa} \bar{\chi}^\nu$. The key idea is that because they measure an isolated black hole, $\bar{\kappa}$ is in fact the surface gravity of an isolated black hole; any possible tidal corrections scale with the square of the small mass and are negligible in the test particle limit. All of the above considerations hold for comparable mass systems so long as the radius of curvature \mathcal{R} due to external influences on each of the holes is large compared to the size of the hole, $\mathcal{R} \gg m_i$.

The relation (3) between z_i and κ_i can be made rigorous in a HKV spacetime using matched asymptotic expansions [37] and is straightforward to demonstrate in the context of isolated boosted black holes and black holes immersed in an axisymmetric external potential. Equation (3) allows us to compare analytic predictions of z to κ of the corresponding black hole in a simulation, although we expect it will begin to break down when the system becomes very relativistic, except on the smaller hole when $q \ll 1$.

However, Eq. (3) relies on the normalization of χ^μ in terms of K^μ and the asymptotic observers, in particular $\chi^t = 1$. In a numerical spacetime, we do not have access to the properly normalized χ^μ . Instead, we measure the tangents l^μ with some unknown normalization, and a corresponding $\kappa_{(l)}$ given by $l^\mu \nabla_\mu l^\nu = \kappa_{(l)} l^\nu$. We have $l^\mu = \alpha \chi^\mu$ for some factor α . The surface gravity inherits this rescaling, $\kappa_{(l)} = \alpha \kappa$. The unknown α therefore cancels out of the ratio $\kappa_{(l)}/l^t = \kappa/\chi^t = \kappa$, where we have suppressed the subscripts labeling the holes. Using Eq. (3) we arrive at an expression for z which is invariant under a rescaling of l^μ ,

$$z = \frac{\kappa_{(l)}}{l^t \bar{\kappa}}. \quad (4)$$

This expression also accounts for a rescaling of the time coordinate of the form $t \rightarrow \tilde{t}(t)$.

Generally, in numerical spacetimes we do not have access to the horizon generators, but only to the apparent horizons (AHs) on each time slice. The AHs are, however, good approximations to the event horizons (EHs) until near the merger [38]. As such, we use the outward null normal l^μ to the AH to evaluate (4). We compute z

for every horizon tangent in our simulation, and average z over the horizon for our final result. This allows for a different rescaling of each tangent vector, and mitigates the influence of any tidal effects contaminating κ .

Approximate helical symmetry and expected errors.—In order to make any sense of (2) in an actual quasi-circular inspiral, we must assume that this relation holds when the HKV is only approximate. We imagine that the binary inspirals adiabatically, passing from circular orbit to circular orbit. At each stage, a small region of spacetime volume enclosing the binary can be approximated by the appropriate HKV spacetime. These regions are connected to asymptotic infinity by null surfaces, and radiation propagating on these surfaces inherits the approximate HKV, connecting each region to infinity. It is clear from these considerations that we should use the Bondi mass and angular momentum in (2), which are constant on each asymptotic null surface but vary as the inspiral proceeds and the approximate HKV evolves [18]. Making this argument rigorous in the sense of a two-timescale expansion [39, 40] is an open problem, and our results provide evidence that this can be done.

With this picture in mind, we can estimate the expected sources of error which will prevent (2) from holding exactly. Since the HKV is only approximate, Killing's equation is violated: $\nabla_{(\mu} l_{\nu)} \neq 0$. This will generate a shear $\sigma_{\mu\nu}$ of the null generators, which in turn represents gravitational waves which enter the horizon and increase its mass [41], giving the estimate $\dot{m} \sim |\sigma|^2$. In practice our simulations have $\dot{m} \sim 10^{-9}$ and so $|\sigma| \sim 10^{-5}$. Conservatively, non-adiabatic effects can be expected to scale as $\dot{\Omega}/(2\Omega^2)$ which is typically $10^{-2} - 10^{-3}$ until close to merger. Another source of error is the fact that only corotating binaries have a strict HKV, but this condition cannot be satisfied for an inspiral where the orbital frequency evolves. We would naively require $\Omega_H \sim \Omega$, and errors for our nonspinning configurations which scale as $\Omega_H^2 \sim \Omega^2 \sim 10^{-2} - 10^{-4}$, although studies of initial data configurations indicate a smaller error in practice [42]. A source of error during the final plunge and merger is the use of AHs rather than the EH. Before plunge, we expect the AH and EH to be identical, since the EH generators approach the AH exponentially fast as we move backward in time from merger, with e -folding time $1/\kappa_i$ [38]. The AHs meanwhile are not very dynamic before merger, since \dot{m} is small, and so the generators have no difficulty reaching the AH. We leave a full investigation and possible mitigation of these errors for future study.

Numerical simulations.—We carry out numerical simulations of quasi-circular inspirals at three mass ratios $q = m_2/m_1 = \{1, 2/5, 2/7\}$ using the `SpEC` code [43]. These black hole binaries execute ~ 28 orbits, beginning at an initial orbital frequencies of $m\Omega_0 \approx \{1.22, 1.33, 1.46\} \times 10^{-2}$, where m is the total mass of the spacetime. We use initial parameters for circularized [44, 45] binaries presented in the waveform catalog re-

ported in [46], or from the publicly available catalog [47] reported in [48]. They have initial eccentricities $e < 10^{-4}$ in all cases. We evolve each configuration at $\{5, 2, 2\}$ resolutions. Our numerical error, represented by the difference in measured values across resolutions, is much smaller than the difference between the numerical results and analytic theory for all of our comparisons.

We measure the orbital frequency using the extrapolated gravitational waveforms [49–51], by defining $\Omega(t) = \omega_{22}(t_r)/2$, where ω_{22} is the frequency of the $l = m = 2$ mode of the gravitational waveform. Local and asymptotic quantities are compared using the corresponding retarded time $t_r = t - r_*$ for the waveform, with r_* a tortoise coordinate defined with respect to the initial ADM mass of the spacetime [50]. In [46, 52] waveform extrapolation has been compared to the more sophisticated procedure of Cauchy Characteristic Extraction [53, 54]; those studies indicate that any systematic errors introduced by extrapolation are small enough that we neglect them in our discussion below.

We use t_r to propagate the asymptotic frequency to the location of the black holes; this captures most of the expected relativistic effects, but given the precision of our comparison further study of this matching is warranted. Local and asymptotic quantities $f(\Omega)$ are compared to PN predictions at equal orbital frequencies, $\Omega_{\text{orb}} = \Omega$. While the orbital frequency of the PN binary is not strictly equal to $\omega_{22}/2$, the corrections to this relation enter at a relative 5PN order and so we neglect them here. The extrapolated waveform is used to compute the energy and angular momentum fluxes from the simulation at each time step, and the Bondi quantities are computed by subtracting the integrated flux [49] from the initial ADM mass and angular momentum of the spacetime, $M_B(t_r) = M_{\text{ADM}} - \int_0^{t_r} dt \dot{E}$ and similarly for J_B .

We measure the redshift factor in Eq. (4) using the outward null normals l^μ of the AH, and using the area of the AH to compute the irreducible mass. We also monitor the spins of the black holes computed using the approximate Killing vector method [55], and they remain negligible, $S_i/m_i^2 \lesssim \{1, 7, 7\} \times 10^{-5}$, until very near merger.

Results.—In Fig. 2 we plot $z(\Omega)$ for all resolutions of our three binary systems (solid lines) together with the 3PN analytic prediction (dashed lines) of [18] and the test particle limit. We indicate the ISCO frequency for a Schwarzschild black hole of total mass m by the vertical dashed line in all our plots, which we cut off shortly before a common horizon forms. We see the general trend of z decreasing from unity as the binaries inspiral. The trend can be understood by considering the test particle limit $z = \sqrt{1 - 3(m\Omega)^{2/3}}$, and by noting that the less massive black holes have a stronger redshift effect due to the deeper gravitational potential of the more massive hole.

Figure 3 shows the differences $\Delta z = z_{\text{NR}} - z_{\text{PN}}$ between numerical and PN predictions for z . We see re-

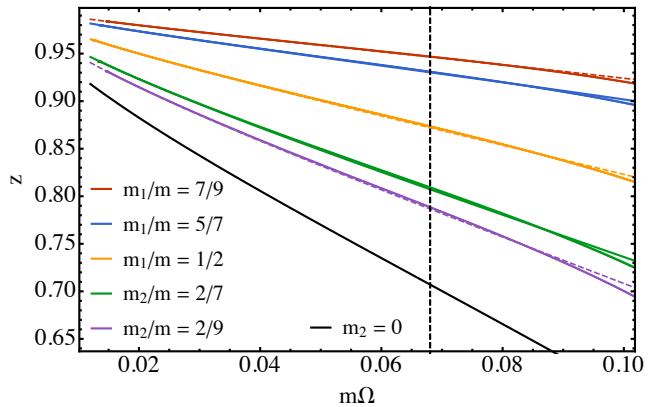


FIG. 2. Redshift plotted for three binary inspirals with $q = \{1, 2/5, 2/7\}$ (solid lines) together with the 3PN prediction (dashed lines). Multiple resolutions are plotted in each case, with five resolutions for $q = 1$ and two resolutions for each of $q = 2/5$ and $q = 2/7$.

markable agreement with the PN predictions in all cases even through the beginning of plunge, with the agreement better for more massive black holes. The small oscillations seen in the lower q systems can be attributed to small residual eccentricities, which are a factor of ~ 4 larger than the $q = 1$ case. Our numerical errors are several times smaller than Δz in all cases at all frequencies. We note that the difference between the 2PN and 3PN predictions are also quite small for these binaries, less than or comparable to Δz .

Finally, we present a test of the first law, Eq. (2). We plot the difference $\Delta Q = z_1 m_1 + z_2 m_2 - (M_B - 2\Omega J_B)$ in Fig. 4. The difference is dominated by Δz in all cases, resulting in similar deviations as in Fig. 3. We emphasize that this comparison is sensitive to many aspects of the conjectured relation (2) as applied to binary inspirals. These include the mapping at retarded times between local and global quantities, the degree to which non-adiabatic effects spoil the first law, and the use of Bondi quantities instead of the ADM quantities used by analytic derivations of the first law (an important exception is [25]). In this sense, the close agreement is remarkable, and may improve further if those errors which can be controlled are dealt with. This agreement even into the plunge phase indicates that the first law or some correction to it may be of use in evolving the binary beyond the slow inspiral regime studied by analytic approximations.

We have also checked that following ringdown, the redshift factor of the final black hole approaches unity when the reference surface gravity $\bar{\kappa}$ is taken to be that of a Kerr black hole with the appropriate mass and spin.

Discussion.—We have presented the first extraction of the redshift factor z from numerical simulations of binary black hole inspirals, by exploiting a connection between this quantity and the appropriately normalized surface

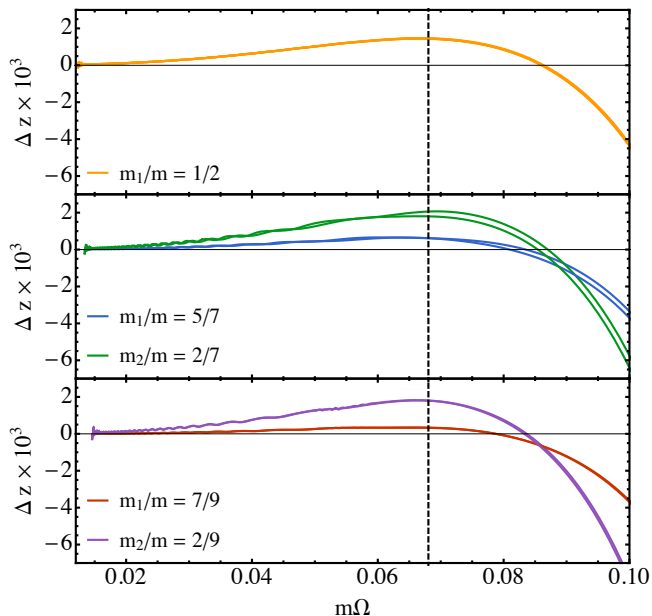


FIG. 3. Differences between the PN predictions for z and the numerical values of z in Fig. 2 for our three binary inspirals, $q = 1$ (top panel), $q = 2/5$ (middle panel) and $q = 2/7$ (bottom panel). As in Fig. 2 multiple resolutions are plotted in each case, although they are not distinguishable for the equal mass binary.

gravity of the black hole. We have shown that the resulting z is in good agreement with PN theory for several mass ratios. Finally, we have performed the first test of the first law of black hole binaries in the non-adiabatic regime, finding surprising agreement between our simulations and analytic predictions.

The results presented here are the first step towards a variety of future interactions between numerical simulations and analytic methods. As a first step we will apply our methods to the study of binaries at high mass ratios, allowing for a test of the regime of validity of the SF approximation and the possible extraction of higher order SF terms [56]. Following this, we can explore spinning [24, 57] and eccentric [58, 59] simulations, for which modified first laws hold. A second natural direction of study is to investigate the redshift factor on the actual event horizons of black hole spacetimes, although this requires intensive post-processing [60, 61]. As an alternative, one could improve the extraction of the redshift by developing a method to compute the best approximate HKV at each time step, in the spirit of the method used in SpEC to compute black hole spins [55, 62–64]. Finally, our results motivate further formal studies of spacetimes which possess an approximate HKV.

Looking towards the future, we envision z as one member of a family of invariant quantities which can be extracted from simulations and used to interconnect between analytic theory, waveform models, and full simula-

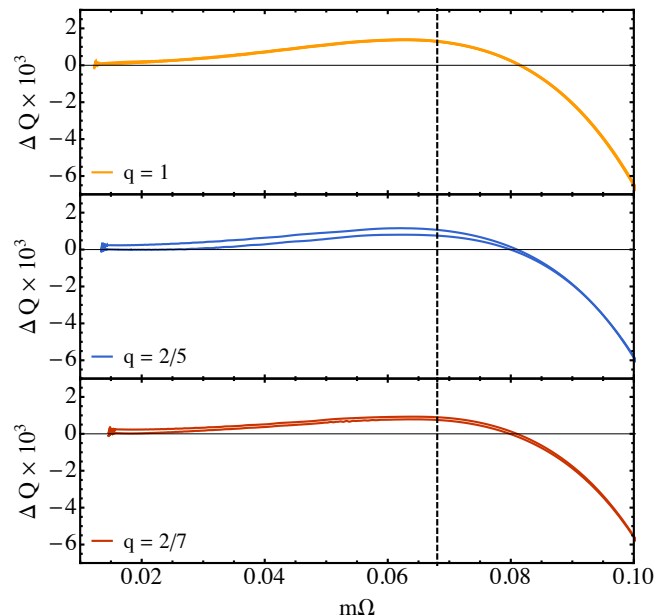


FIG. 4. Deviation from the integral relation (2) from the first law, for each of our three binary inspirals: $q = 1$ (top panel), $q = 2/5$ (middle panel) and $q = 2/7$ (bottom panel). As in Fig. 2 multiple resolutions are plotted in each case, although they are not distinguishable for the equal mass binary.

tions. As we continue to refine our understanding of the relativistic two-body problem, these insights will transfer to the understanding of gravitational wave emission from these systems, and in turn improve our ability to draw astrophysical insights from compact binaries in the nascent era of gravitational wave astronomy.

Acknowledgements:— We thank Takahiro Tanaka for first suggesting this method for computing the redshift factor in numerical spacetimes. This work was conceived at the 18th Capra meeting and molecule workshop YITP-T-15-3 at the Yukawa Institute for Theoretical Physics. We thank the participants of this conference for valuable discussions, especially Takahiro Tanaka, Alexandre Le Tiec, Adam Pound, and Leor Barack. We also thank Abraham Harte, Ian Hinder, Soichiro Isoyama, and Eric Poisson for valuable discussions, Serguei Ossokine for assistance in computing the energy and angular momentum fluxes to infinity, Tony Chu for providing circularized initial data parameters for some of our simulations, and Adam Pound for valuable comments on this manuscript. Calculations were performed using the Spectral Einstein code (SpEC) [43]. We gratefully acknowledge funding from NSERC of Canada, the Ontario Early Researcher Awards Program, the Canada Research Chairs Program, and the Canadian Institute for Advanced Research; AZ was supported by the Beatrice and Vincent Tremaine Postdoctoral Fellowship at the Canadian Institute for Theoretical Astrophysics during a portion of this work. Computations were performed on the GPC super-

computer at the SciNet HPC Consortium [65]. SciNet is funded by: the Canada Foundation for Innovation under the auspices of Compute Canada; the Government of Ontario; Ontario Research Fund - Research Excellence; and the University of Toronto.

-
- [1] B. P. Abbott *et al.* (Virgo, LIGO Scientific), “Observation of Gravitational Waves from a Binary Black Hole Merger,” *Phys. Rev. Lett.* **116**, 061102 (2016), [arXiv:1602.03837 \[gr-qc\]](#).
 - [2] B. P. and others Abbott (Virgo, LIGO Scientific), “GW151226: Observation of Gravitational Waves from a 22-Solar-Mass Binary Black Hole Coalescence,” *Phys. Rev. Lett.* **116**, 241103 (2016), [arXiv:1606.04855 \[gr-qc\]](#).
 - [3] “Binary Black Hole Mergers in the first Advanced LIGO Observing Run,” (2016), [arXiv:1606.04856 \[gr-qc\]](#).
 - [4] Luc Blanchet, “Gravitational Radiation from Post-Newtonian Sources and Inspiralling Compact Binaries,” *Living Rev. Rel.* **17**, 2 (2014), [arXiv:1310.1528 \[gr-qc\]](#).
 - [5] Eric Poisson, Adam Pound, and Ian Vega, “The Motion of point particles in curved spacetime,” *Living Rev. Rel.* **14**, 7 (2011), [arXiv:1102.0529 \[gr-qc\]](#).
 - [6] Harald P. Pfeiffer, “Numerical simulations of compact object binaries,” *Gravitational waves. Numerical relativity - data analysis. Proceedings, 9th Edoardo Amaldi Conference, Amaldi 9, and meeting, NRDA 2011, Cardiff, UK, July 10-15, 2011, Class. Quant. Grav.* **29**, 124004 (2012), [arXiv:1203.5166 \[gr-qc\]](#).
 - [7] Ian Hinder *et al.*, “Error-analysis and comparison to analytical models of numerical waveforms produced by the NRAR Collaboration,” *Class. Quant. Grav.* **31**, 025012 (2014), [arXiv:1307.5307 \[gr-qc\]](#).
 - [8] Matthew W. Choptuik, Luis Lehner, and Frans Pretorius, “Probing Strong Field Gravity Through Numerical Simulations,” (2015), [arXiv:1502.06853 \[gr-qc\]](#).
 - [9] A. Buonanno and T. Damour, “Effective one-body approach to general relativistic two-body dynamics,” *Phys. Rev. D* **59**, 084006 (1999), [arXiv:gr-qc/9811091 \[gr-qc\]](#).
 - [10] Alessandra Buonanno and Thibault Damour, “Transition from inspiral to plunge in binary black hole coalescences,” *Phys. Rev. D* **62**, 064015 (2000), [arXiv:gr-qc/0001013 \[gr-qc\]](#).
 - [11] Mark Hannam, Patricia Schmidt, Alejandro Bohé, Leïla Haegel, Sascha Husa, Frank Ohme, Geraint Pratten, and Michael Pürrer, “Simple Model of Complete Precessing Black-Hole-Binary Gravitational Waveforms,” *Phys. Rev. Lett.* **113**, 151101 (2014), [arXiv:1308.3271 \[gr-qc\]](#).
 - [12] Alexandre Le Tiec, Abdul H. Mroue, Leor Barack, Alessandra Buonanno, Harald P. Pfeiffer, Norichika Sago, and Andrea Taracchini, “Periastron Advance in Black Hole Binaries,” *Phys. Rev. Lett.* **107**, 141101 (2011), [arXiv:1106.3278 \[gr-qc\]](#).
 - [13] Alexandre Le Tiec, “The Overlap of Numerical Relativity, Perturbation Theory and Post-Newtonian Theory in the Binary Black Hole Problem,” *Int. J. Mod. Phys. D* **23**, 1430022 (2014), [arXiv:1408.5505 \[gr-qc\]](#).
 - [14] Steven L. Detweiler, “A Consequence of the gravitational self-force for circular orbits of the Schwarzschild geometry,” *Phys. Rev. D* **77**, 124026 (2008), [arXiv:0804.3529 \[gr-qc\]](#).
 - [15] Norichika Sago, Leor Barack, and Steven L. Detweiler, “Two approaches for the gravitational self force in black hole spacetime: Comparison of numerical results,” *Phys. Rev. D* **78**, 124024 (2008), [arXiv:0810.2530 \[gr-qc\]](#).
 - [16] Abhay G. Shah, Tobias S. Keidl, John L. Friedman, Dong-Hoon Kim, and Larry R. Price, “Conservative, gravitational self-force for a particle in circular orbit around a Schwarzschild black hole in a Radiation Gauge,” *Phys. Rev. D* **83**, 064018 (2011), [arXiv:1009.4876 \[gr-qc\]](#).
 - [17] Luc Blanchet, Steven L. Detweiler, Alexandre Le Tiec, and Bernard F. Whiting, “High-Order Post-Newtonian Fit of the Gravitational Self-Force for Circular Orbits in the Schwarzschild Geometry,” *Phys. Rev. D* **81**, 084033 (2010), [arXiv:1002.0726 \[gr-qc\]](#).
 - [18] Alexandre Le Tiec, Luc Blanchet, and Bernard F. Whiting, “The First Law of Binary Black Hole Mechanics in General Relativity and Post-Newtonian Theory,” *Phys. Rev. D* **85**, 064039 (2012), [arXiv:1111.5378 \[gr-qc\]](#).
 - [19] Donato Bini and Thibault Damour, “Analytical determination of the two-body gravitational interaction potential at the fourth post-Newtonian approximation,” *Phys. Rev. D* **87**, 121501 (2013), [arXiv:1305.4884 \[gr-qc\]](#).
 - [20] Jacob D. Bekenstein, “Black holes and entropy,” *Phys. Rev. D* **7**, 2333–2346 (1973).
 - [21] James M. Bardeen, B. Carter, and S. W. Hawking, “The Four laws of black hole mechanics,” *Commun. Math. Phys.* **31**, 161–170 (1973).
 - [22] S. W. Hawking, “Particle Creation by Black Holes,” *In *Gibbons, G.W. (ed.), Hawking, S.W. (ed.): Euclidean quantum gravity* 167-188, Commun. Math. Phys.* **43**, 199–220 (1975), [167(1975)].
 - [23] John L. Friedman, Koji Uryu, and Masaru Shibata, “Thermodynamics of binary black holes and neutron stars,” *Phys. Rev. D* **65**, 064035 (2002), [Erratum: *Phys. Rev. D* **70**, 129904(2004)], [arXiv:gr-qc/0108070 \[gr-qc\]](#).
 - [24] Luc Blanchet, Alessandra Buonanno, and Alexandre Le Tiec, “First law of mechanics for black hole binaries with spins,” *Phys. Rev. D* **87**, 024030 (2013), [arXiv:1211.1060 \[gr-qc\]](#).
 - [25] Samuel E. Gralla and Alexandre Le Tiec, “Thermodynamics of a Black Hole with Moon,” *Phys. Rev. D* **88**, 044021 (2013), [arXiv:1210.8444 \[gr-qc\]](#).
 - [26] Soichiro Isoyama, Leor Barack, Sam R. Dolan, Alexandre Le Tiec, Hiroyuki Nakano, Abhay G. Shah, Takahiro Tanaka, and Niels Warburton, “Gravitational Self-Force Correction to the Innermost Stable Circular Equatorial Orbit of a Kerr Black Hole,” *Phys. Rev. Lett.* **113**, 161101 (2014), [arXiv:1404.6133 \[gr-qc\]](#).
 - [27] Donato Bini and Thibault Damour, “High-order post-Newtonian contributions to the two-body gravitational interaction potential from analytical gravitational self-force calculations,” *Phys. Rev. D* **89**, 064063 (2014), [arXiv:1312.2503 \[gr-qc\]](#).
 - [28] Donato Bini and Thibault Damour, “Conservative second-order gravitational self-force on circular orbits and the effective one-body formalism,” *Phys. Rev. D* **93**, 104040 (2016), [arXiv:1603.09175 \[gr-qc\]](#).
 - [29] J. Aasi *et al.* (LIGO Scientific), “Advanced LIGO,” *Class. Quant. Grav.* **32**, 074001 (2015), [arXiv:1411.4547 \[gr-qc\]](#).
 - [30] B. P. Abbott *et al.* (Virgo, LIGO Scientific), “GW150914: First results from the search for binary black hole coalescence with Advanced LIGO,” (2016), [arXiv:1602.03839 \[gr-qc\]](#).
 - [31] B. P. Abbott *et al.* (Virgo, LIGO Scientific), “Properties

- of the binary black hole merger GW150914,” (2016), [arXiv:1602.03840 \[gr-qc\]](#).
- [32] Thibault Damour, Alessandro Nagar, Denis Pollney, and Christian Reisswig, “Energy versus Angular Momentum in Black Hole Binaries,” *Phys. Rev. Lett.* **108**, 131101 (2012), [arXiv:1110.2938 \[gr-qc\]](#).
- [33] Alexandre Le Tiec, Enrico Barausse, and Alessandra Buonanno, “Gravitational Self-Force Correction to the Binding Energy of Compact Binary Systems,” *Phys. Rev. Lett.* **108**, 131103 (2012), [arXiv:1111.5609 \[gr-qc\]](#).
- [34] Alessandro Nagar, Thibault Damour, Christian Reisswig, and Denis Pollney, “Energetics and phasing of non-precessing spinning coalescing black hole binaries,” *Phys. Rev.* **D93**, 044046 (2016), [arXiv:1506.08457 \[gr-qc\]](#).
- [35] Robert M. Wald, “Black hole entropy is the Noether charge,” *Phys. Rev.* **D48**, 3427–3431 (1993), [arXiv:gr-qc/9307038 \[gr-qc\]](#).
- [36] Steven L. Detweiler, “Radiation reaction and the selfforce for a point mass in general relativity,” *Phys. Rev. Lett.* **86**, 1931–1934 (2001), [arXiv:gr-qc/0011039 \[gr-qc\]](#).
- [37] Adam Pound, “Self-force effects on the horizon geometry of a small black hole,” (2015), unpublished.
- [38] Michael I. Cohen, Harald P. Pfeiffer, and Mark A. Scheel, “Revisiting Event Horizon Finders,” *Class. Quant. Grav.* **26**, 035005 (2009), [arXiv:0809.2628 \[gr-qc\]](#).
- [39] Tanja Hinderer and Eanna E. Flanagan, “Two timescale analysis of extreme mass ratio inspirals in Kerr. I. Orbital Motion,” *Phys. Rev.* **D78**, 064028 (2008), [arXiv:0805.3337 \[gr-qc\]](#).
- [40] Adam Pound, “Second-order perturbation theory: problems on large scales,” *Phys. Rev.* **D92**, 104047 (2015), [arXiv:1510.05172 \[gr-qc\]](#).
- [41] S. W. Hawking and J. B. Hartle, “Energy and angular momentum flow into a black hole,” *Commun. Math. Phys.* **27**, 283–290 (1972).
- [42] Matthew Caudill, Gregory B. Cook, Jason D. Grigsby, and Harald P. Pfeiffer, “Circular orbits and spin in black-hole initial data,” *Phys. Rev.* **D74**, 064011 (2006), [arXiv:gr-qc/0605053 \[gr-qc\]](#).
- [43] <http://www.black-holes.org/SpEC.html>.
- [44] Abdul H. Mroue, Harald P. Pfeiffer, Lawrence E. Kidder, and Saul A. Teukolsky, “Measuring orbital eccentricity and periastron advance in quasi-circular black hole simulations,” *Phys. Rev.* **D82**, 124016 (2010), [arXiv:1004.4697 \[gr-qc\]](#).
- [45] Alessandra Buonanno, Lawrence E. Kidder, Abdul H. Mroue, Harald P. Pfeiffer, and Andrea Taracchini, “Reducing orbital eccentricity of precessing black-hole binaries,” *Phys. Rev.* **D83**, 104034 (2011), [arXiv:1012.1549 \[gr-qc\]](#).
- [46] Tony Chu, Heather Fong, Prayush Kumar, Harald P. Pfeiffer, Michael Boyle, Daniel A. Hemberger, Lawrence E. Kidder, Mark A. Scheel, and Bela Szilagyi, “On the accuracy and precision of numerical waveforms: Effect of waveform extraction methodology,” (2015), [arXiv:1512.06800 \[gr-qc\]](#).
- [47] <http://www.black-holes.org/waveforms>.
- [48] Abdul H. Mroue *et al.*, “Catalog of 174 Binary Black Hole Simulations for Gravitational Wave Astronomy,” *Phys. Rev. Lett.* **111**, 241104 (2013), [arXiv:1304.6077 \[gr-qc\]](#).
- [49] Michael Boyle, Alessandra Buonanno, Lawrence E. Kidder, Abdul H. Mroue, Yi Pan, Harald P. Pfeiffer, and Mark A. Scheel, “High-accuracy numerical simulation of black-hole binaries: Computation of the gravitational-wave energy flux and comparisons with post-Newtonian approximants,” *Phys. Rev.* **D78**, 104020 (2008), [arXiv:0804.4184 \[gr-qc\]](#).
- [50] Michael Boyle and Abdul H. Mroue, “Extrapolating gravitational-wave data from numerical simulations,” *Phys. Rev.* **D80**, 124045 (2009), [arXiv:0905.3177 \[gr-qc\]](#).
- [51] Michael Boyle, “Angular velocity of gravitational radiation from precessing binaries and the corotating frame,” *Phys. Rev.* **D87**, 104006 (2013), [arXiv:1302.2919 \[gr-qc\]](#).
- [52] Nicholas W. Taylor, Michael Boyle, Christian Reisswig, Mark A. Scheel, Tony Chu, Lawrence E. Kidder, and Béla Szilágyi, “Comparing Gravitational Waveform Extrapolation to Cauchy-Characteristic Extraction in Binary Black Hole Simulations,” *Phys. Rev.* **D88**, 124010 (2013), [arXiv:1309.3605 \[gr-qc\]](#).
- [53] Nigel T. Bishop, Roberto Gomez, Luis Lehner, and Jeffrey Winicour, “Cauchy characteristic extraction in numerical relativity,” *Phys. Rev.* **D54**, 6153–6165 (1996).
- [54] M. C. Babiuc, B. Szilagyi, J. Winicour, and Y. Zlochower, “A Characteristic Extraction Tool for Gravitational Waveforms,” *Phys. Rev.* **D84**, 044057 (2011), [arXiv:1011.4223 \[gr-qc\]](#).
- [55] Geoffrey Lovelace *et al.*, “Nearly extremal apparent horizons in simulations of merging black holes,” *Class. Quant. Grav.* **32**, 065007 (2015), [arXiv:1411.7297 \[gr-qc\]](#).
- [56] Aaron Zimmerman, Adam G. M. Lewis, and Harald Pfeiffer, “Redshift factor in numerical simulations,” (2016), in preparation.
- [57] Abhay G. Shah, John L. Friedman, and Tobias S. Keidl, “Extreme-mass-ratio inspiral corrections to the angular velocity and redshift factor of a mass in circular orbit about a Kerr black hole,” *Phys. Rev.* **D86**, 084059 (2012), [arXiv:1207.5595 \[gr-qc\]](#).
- [58] Alexandre Le Tiec, “First Law of Mechanics for Compact Binaries on Eccentric Orbits,” *Phys. Rev.* **D92**, 084021 (2015), [arXiv:1506.05648 \[gr-qc\]](#).
- [59] Maarten van de Meent and Abhay G. Shah, “Metric perturbations produced by eccentric equatorial orbits around a Kerr black hole,” *Phys. Rev.* **D92**, 064025 (2015), [arXiv:1506.04755 \[gr-qc\]](#).
- [60] Michael I. Cohen, Jeffrey D. Kaplan, and Mark A. Scheel, “On Toroidal Horizons in Binary Black Hole Inspirals,” *Phys. Rev.* **D85**, 024031 (2012), [arXiv:1110.1668 \[gr-qc\]](#).
- [61] Andy Bohn, Lawrence E. Kidder, and Saul A. Teukolsky, “A Parallel Adaptive Event Horizon Finder for Numerical Relativity,” (2016), [arXiv:1606.00437 \[gr-qc\]](#).
- [62] Gregory B. Cook and Bernard F. Whiting, “Approximate Killing Vectors on S^{*2} ,” *Phys. Rev.* **D76**, 041501 (2007), [arXiv:0706.0199 \[gr-qc\]](#).
- [63] Geoffrey Lovelace, Robert Owen, Harald P. Pfeiffer, and Tony Chu, “Binary-black-hole initial data with nearly-extremal spins,” *Phys. Rev.* **D78**, 084017 (2008), [arXiv:0805.4192 \[gr-qc\]](#).
- [64] Christopher Beetle, “Approximate Killing Fields as an Eigenvalue Problem,” (2008), [arXiv:0808.1745 \[gr-qc\]](#).
- [65] Chris Loken, Daniel Gruner, Leslie Groer, Richard Peltier, Neil Bunn, Michael Craig, Teresa Henriques, Jillian Dempsey, Ching-Hsing Yu, Joseph Chen, L Jonathan Dursi, Jason Chong, Scott Northrup, Jaime Pinto, Neil Knecht, and Ramses Van Zon, “Scinet: Lessons learned from building a power-efficient top-20 system and data centre,” *Journal of Physics: Conference Series* **256**, 012026 (2010).